Available online at www.sciencedirect.com

SCIENCE DIRECT®

Biochimica et Biophysica Acta 1608 (2004) 23–33

BIOCHIMICA ET BIOPHYSICA ACTA

BBA

www.bba-direct.com

Heme protein films with polyamidoamine dendrimer: direct electrochemistry and electrocatalysis

Li Shen, Naifei Hu*

Department of Chemistry, Beijing Normal University, Beijing 100875, China

Received 26 June 2003; received in revised form 29 September 2003; accepted 10 October 2003

Abstract

Biocompatible nanosized polyamidoamine (PAMAM) dendrimer films provided a suitable microenvironment for heme proteins to transfer electron directly with underlying pyrolytic graphite (PG) electrodes. Hemoglobin (Hb), myoglobin (Mb), horseradish peroxidase (HRP), and catalase (Cat) incorporated in PAMAM films exhibited a pair of well-defined, quasi-reversible cyclic voltammetric peaks, respectively, characteristic of the protein heme Fe(III)/Fe(II) redox couples. While Hb-, Mb-, and HRP-PAMAM films showed the cyclic voltammetry (CV) peaks at about −0.34 V vs. saturated calomel electrode (SCE) in pH 7.0 buffers, Cat-PAMAM films displayed the peak pair at a more negative potential of −0.47 V. The protein-PAMAM films demonstrated a surface-confined or thin-layer voltammetric behavior. The electrochemical parameters such as apparent heterogeneous electron transfer rate constants (k_s) and formal potentials ($E^{\circ\prime}$) were estimated by square wave voltammetry with nonlinear regression analysis. UV–vis and IR spectroscopy showed that the proteins retained their near-native secondary structures in PAMAM films. Oxygen, hydrogen peroxide, and nitrite were catalytically reduced at the protein-PAMAM film electrodes, showing the potential applicability of the films as the new type of biosensors or bioreactors based on direct electrochemistry of the proteins.

Keywords: Myoglobin; Hemoglobin; Horseradish peroxidase; Catalase; Polyamidoamine dendrimer; Direct electrochemistry; Electrochemical catalysis

1. Introduction

Over the past decade, several types of redox protein films have been developed to achieve direct electron exchange of proteins or enzymes with electrodes [1,2]. The direct electrochemistry of these protein or enzyme films provides a model for investigating mechanisms of redox transformations between enzyme molecules in biocatalysis and metabolic processes involving electron transportation in biological systems [3]. For example, one of our particular interests is to develop stable films for studying chemical pollutant activation catalyzed by the family of iron heme cytochrome P450 (Cyt P450) enzymes [4]. Since Cyt P450s are not commercially available and require considerable effort to obtain, our approach has been to develop films using the other easy-to-get heme proteins such as myoglobin (Mb), hemoglobin (Hb), or horseradish peroxidase (HRP) as an experimental model [5].

The direct electrochemistry of protein films can also establish a foundation for constructing the third generation of electrochemical biosensors [6] and a new kind of bioreactors, in which the redox mediators are no longer needed, and the complications brought about by the mediators are avoided. Immobilization of proteins or enzymes is one of the key steps in fabricating biosensors or bioreactors. Our long-term goal is to develop stable protein films with good electroactivity and enzyme activity. Various types of films have been developed to immobilize proteins and achieve direct electrochemistry and electrocatalysis. Several examples include cast films of proteins with insoluble surfactants [7,8], hydrogel polymers [9–11] or biopolymers [12,13], polyelectrolyte- or clay-surfactant composites [14–16], and films of proteins and polyions grown layer-by-layer [17–19]. Recently, efforts have been devoted to construction of protein films either cast or layer-by-layer assembled on electrodes with nanoparticles such as MnO_2, SiO_2 or exfoliated clay [20–22]. Inorganic nanoparticle films demon-

* Corresponding author. Fax: +86-10-6220-0567.
E-mail address: hunaifei@bnu.edu.cn (N. Hu).

0005-2728/$ - see front matter © 2003 Elsevier B.V. All rights reserved.
doi:10.1016/j.bbabio.2003.10.007

strate unique and excellent properties including good biocompatibility, high surface activity, and nice stability when used to immobilize proteins or enzymes. All these films enhance the direct, quasi-reversible electron transfer between heme proteins and electrodes compared to that on bare electrodes with the proteins in solution.

In recent years, dendrimers, a new class of polymers, have aroused great interest and has been used as a building unit for constructing the organic nanostructure films [23,24]. Dendrimers have a highly branched dendritic structure, and possess some excellent characteristics such as a high density of active groups, good structural homogeneity, and intense internal porosity [23,25,26]. For instance, the fourth generation polyamidoamine (PAMAM) dendrimer possesses 64 primary amine groups on the surface and has a spherical shape with diameter of about 4.5 nm [23,27]. In aqueous solution, PAMAM can be protonated at its terminal and/or internal amino groups depending on the solution pH [28].

PAMAM dendrimers are of particular interest because their polyamidoamine structure mimicking the three-dimensional structure of biomacromolecules and their good biocompatibility [29,30]. PAMAM has thus been utilized as the bioconjugating reagents for construction of films with biomolecules. For instance, Kim et al. [31,32] developed a glucose biosensor prepared by alternate layer-by-layer depositions of periodate-oxidized glucose oxidase (GOX) and PAMAM or ferrocenyl-tethered PAMAM. They also constructed a biosensor based on avidin–biotin affinity interaction in which a PAMAM monolayer functionalized with ferrocenyl and biotin analogues was assembled layer-by-layer on gold electrodes [33]. Biotinylated GOX as a model enzyme was also loaded onto the affinity surface of PAMAM layers, and cyclic voltammetric measurements were performed by registering the activity of the associated GOX [34]. The unique and excellent properties of PAMAM, especially its biocompatibility, stimulate us to use this new type of polymers and organic nanoparticles as a building block or film-forming material in preparing protein films on electrodes. We expect that incorporated heme proteins would be compatible with PAMAM in the films and demonstrate good electroactivity and catalytic reactivity. To the best of our knowledge, direct electrochemistry of heme proteins immobilized in PAMAM dendrimer films has not been reported until now.

In the present paper, the simple cast method was used to immobilize heme proteins (Hb, Mb, HRP, and Cat) into PAMAM films on pyrolytic graphite (PG) electrodes. All four protein-PAMAM films showed a quasi-reversible cyclic voltammetric peak pair for the heme Fe(III)/Fe(II) redox couples, respectively. The films were characterized by electrochemical and spectroscopic techniques. Various substrates with biological or environmental significance were electrochemically catalyzed by the protein-PAMAM films. The potential application of the films as a foundation of the new type of biosensor or bioreactor was explored.

2. Materials and methods

2.1. Reagents

The forth generation amine-terminated PAMAM (MW 14,215) were purchased from Aldrich. Mb (MW 17,800) and bovine liver catalase (Cat, EC 1.11.1.6, MW 240,000) were from Sigma. Hb (MW 66,000) and HRP (EC 1.11.1.7, MW 42,100) were obtained from Shanghai Chemical Reagent Company. They were used as received. All other chemicals were reagent grade. $NaNO_2$ and H_2O_2 were freshly prepared before being used.

Buffers were 0.1 M sodium acetate, 0.05 M sodium dihydrogen phosphate, 0.05 M boric acid, or 0.05 M citric acid, all containing 0.1 M KBr. Buffer pH was adjusted with HCl or NaOH solutions. Twice-distilled water was used to prepare solutions.

2.2. Preparation of protein-PAMAM films

Prior to coating, basal plane PG disk (Advanced Ceramics, geometric area 0.16 cm^2) electrodes were abraded with metallographic sandpaper of 1200 grit, and then ultrasonicated in pure water for 30 s. To obtain the best cyclic voltammetric responses, the experimental conditions for film casting, such as the concentration of proteins and PAMAM, the volume ratio of protein/PAMAM, and the total volume of protein-PAMAM solutions, were optimized. Typically, 10 μl of the solution containing 1 mg ml^{-1} PAMAM and 8.5×10^{-6} M Hb, 2.8×10^{-5} M Mb, 1.4×10^{-4} M HRP, or 3.3×10^{-5} M Cat were spread evenly onto a freshly abraded PG electrode. A small bottle was fit tightly over the electrode so that water was evaporated slowly and more uniform films were formed. The films were then dried overnight in air.

2.3. Measurements

Cyclic voltammetry (CV) and square wave voltammetry (SWV) were performed with a CHI 660 electrochemical workstation (CH Instruments). The experiments were carried out in a three-electrode cell at ambient temperature (18 ± 2 °C). A Pt wire was used as counter electrode, a saturated calomel electrode (SCE) was used as reference electrode, and a PG disk coated with films was acted as working electrode. Voltammetries of protein-PAMAM films were carried out in buffers containing no protein. Buffers were purged with highly purified nitrogen for at least 15 min prior to a series of voltammetric experiments. A nitrogen environment was then kept in the cell by continuously bubbling N_2 during the whole experiment. In the experiments with oxygen, measured volumes of air were injected through solutions via a syringe in a sealed cell which had been previously degassed with purified nitrogen. UV–vis spectroscopy was done with a Cintra 10e UV–visible spectrophotometer (GBC). Sample films for spectroscopy

were prepared by depositing protein-PAMAM solutions onto optical glass slides and then being dried in air. Reflectance absorption infrared (RAIR) spectra of the films were obtained by using an Avatar 360 FT-IR spectrophotometer (Nicolet). Films were prepared by depositing the protein-PAMAM solutions onto aluminum disks.

3. Result and discussion

3.1. Direct electrochemistry of heme proteins in PAMAM films

The electrochemical behavior of the four heme protein-PAMAM films was studied by CV. When protein-PAMAM film electrodes were placed in protein-free pH 7.0 buffers, after several CV scans, a pair of well-defined, quasi-reversible CV peaks was observed at about −0.34 V vs. SCE for Hb-, Mb-, and HRP-PAMAM films, and at −0.47 V for Cat-PAMAM films, respectively (Fig. 1). The peaks were located at the potentials characteristic of the heme Fe(III)/Fe(II) redox couples of the proteins [7,35–37]. No CV peak was observed at plain PAMAM film electrodes in the same potential range. This indicates direct electron transfer between the heme proteins and underlying PG electrodes in the PAMAM film environment. The electrochemical parameters of the four protein-PAMAM films obtained from CV are listed in Table 1 for comparison. While the formal potential ($E^{\circ\prime}$), estimated as a midpoint of CV reduction and oxidation peak potentials, was quite similar for Hb-, Mb-, and HRP-PAMAM films, Cat-PAMAM films showed $E^{\circ\prime}$ value of 130 mV more negative than the others. This indicates that the proteins with the same functional group or redox center may not have the same redox formal potential in the same microenvironment, as also observed in the previous work [12]. The exact reason why Hb, Mb, and HRP showed very similar CV peak positions while Cat exhibited its $E^{\circ\prime}$ value so different than the others in PAMAM films is not known yet, but the observation is consistent with the behavior of protein-chitosan films [12]. Electron exchange was much faster for protein-PAMAM films in blank buffers than that for the proteins in solution at bare PG electrodes. For example, Hb in pH 7.0 buffers showed no CV peaks at bare PG electrodes in the same potential window (Fig. 1a). Thus, PAMAM films must have a great effect on the kinetics of the electrode reaction for the proteins and provide a suitable microenvironment for the proteins to transfer electrons with underlying PG electrodes. While the exact nature of this effect is not yet very clear, the role of films in enhancing electron transfer is probably related to the high degree of biocompatibility of PAMAM films [29,30]. Another possibility is that the PAMAM films may inhibit the adsorption of impurities from protein solutions on the electrodes, which could otherwise block electron transfer for the proteins [38].

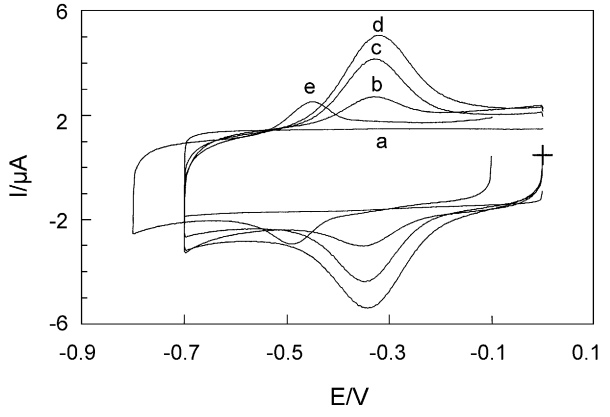

Fig. 1. Cyclic voltammograms at 0.2 V s^{-1} in pH 7.0 buffers for (a) 0.025 mM Hb in buffers at bare PG electrodes, and for (b) HRP-PAMAM, (c) Mb-PAMAM, (d) Hb-PAMAM, and (e) Cat-PAMAM film electrodes.

PAMAM has a unique dendritic architecture in which plenty of internal cavities or voids can host water and small ions when in aqueous buffer solutions [39]. The PAMAM molecule itself has a positive surface charge in pH 7.0 buffer [28]. All these may greatly enhance the conductivity of the PAMAM or protein-PAMAM films in the buffer, and facilitate the electron transfer between the proteins and PG electrodes. PAMAM films with considerable amounts of water provide an essentially aqueous-like microenvironment for proteins, which may also be favorable to the direct electrochemistry of the proteins.

CVs of protein-PAMAM films showed nearly symmetrical peak shapes and roughly equal reduction and oxidation peak currents. The reduction peak currents increased linearly with scan rates in the range from 0.02 to 2 V s^{-1}. Integration of reduction peaks gave nearly constant charge (Q) values with different scan rates. The peak separation (ΔE_p) was only about 20 mV (Table 1) for Hb-, Mb-, and HRP-PAMAM films, much smaller than that of corresponding proteins in other cast films [12,21], while ΔE_p was 40 mV for Cat-PAMAM films. All these results are characteristic of quasi-reversible, surface-confined or thin-layer electrochemical behavior, in which all electroactive proteins in their heme Fe(III) forms in the films are reduced on the forward cathodic scan, and the reduced proteins in their heme Fe(II) forms are then fully oxidized back to the heme Fe(III) forms on the reversed anodic scan [40].

3.2. Stability of protein-PAMAM films

Long-term stability is one of the most important properties required for a biosensor or bioreactor. The stability of protein-PAMAM film electrodes was investigated by CV with two different modes. In the solution studies, a PG electrode modified with protein-PAMAM films was placed in buffers during the whole storage time, and CVs were run periodically. Alternatively, the films were stored in air for most of the storage time, and CVs were run periodically after returning the dry film electrode into buffer solutions.

Table 1
Electrochemical parameters of protein-PAMAM films estimated by CV at pH 7.0

	Molecular weight	Isoelectric point	Deposited Γ/(mol cm^{-2})	Electroactive Γ^*/(mol cm^{-2})[a]	Electroactive protein (%)	$E^{\circ\prime}$/V, vs. SCE[b]	ΔE_p/mV[c]
Hb	66,000	7.4[d]	26.6×10^{-11}	3.7×10^{-11}	13.8	−0.332	17
Mb	17,800	6.8[e]	88.1×10^{-11}	10.4×10^{-11}	11.8	−0.339	16
HRP	42,100	8.9[f]	440×10^{-11}	3.3×10^{-11}	0.8	−0.341	21
Cat	240,000	5.8[g]	105×10^{-11}	0.88×10^{-11}	0.8	−0.469	40

[a] Estimated by integration of CV reduction peak at 0.02–2 V s^{-1}.
[b] Estimated as the midpoint of CV reduction and oxidation peak potentials at 0.2 V s^{-1}.
[c] The peak separation between CV reduction and oxidation peak potentials.
[d] Ref. [44].
[e] Ref. [60].
[f] Ref. [61].
[g] Ref. [62].

Hb-, Mb-, and HRP-PAMAM films demonstrated excellent stability with both methods. The CV peak potentials kept in the same positions during the test, and the peak currents remained essentially unchanged for at least 10 days. Taking Hb-PAMAM films as an example, after 10 days of storage with the "wet method", the CV peak potentials kept in the same positions and the reduction peak current decreased by only about 4%. While with the "dry method", the CV reduction peak current decreased by about 17% in the first 4 days, but then remained constant during the following 6 days of storage, and the peak potentials were always unchanged in the test. However, Cat-PAMAM films were less stable. After soaking in blank buffers for 1 h, the reduction peak current decreased by about 20% compared with the initial steady state, while the peak potentials remained unchanged. Similar situation was also observed in protein-chitosan films, where Cat was much less stable than Hb, Mb, and HRP [12]. In other polymer and lipid films, Hb, Mb, and HRP also showed very good stability [8–10,13–16], while Cat was less stable [11], although the reason is not yet clear.

It is known that PAMAM dendrimers are very hydrophilic and water-soluble [24,25]. Why were the protein-PAMAM films, except Cat-PAMAM, cast on PG surface so stable in aqueous solution? To further investigate the interaction between the protein and PAMAM, a PG disk coated with Hb-PAMAM films was placed into a blank buffer solution of 3 ml at pH 7.0, and the characteristic and sensitive Soret absorption band for Hb at 412 nm in the external solution was monitored with UV–vis spectroscopy. At the first 100 s, the absorbance of Soret band increased rapidly with soaking time, indicating that some Hb in the Hb-PAMAM films did diffuse out from the films. The absorbance grew much slower in the next 100 s, and no longer increased afterwards. When Hb with the same amount as that of deposited on the PG surface (0.3 nmol) was directly dissolved in a 3 ml buffer solution, its absorbance at 412 nm measured by UV–vis spectroscopy would represent the total amount of Hb deposited on PG, and then the fraction of Hb diffusing out from the Hb-PAMAM films could be estimated. The results showed that only about 11% of Hb in the Hb-PAMAM films were lost during the soaking, and after about 200 s of immersing, no further leaking of Hb was observed and the films became quite stable. Thus, the interaction between Hb and PAMAM would make great contribution to the stability of the films in aqueous solution. After being abraded, the surface of basal plane PG became rough and the "edge" surface of PG was uncovered, which was negatively charged by virtue of the surface oxygen functionalities. Thus, positively charged organic PAMAM would strongly interact with PG by electrostatic attraction, which would also strengthen the stability of the protein-PAMAM films on PG.

To further investigate the interaction between the proteins and PAMAM, the PG electrodes coated with plain PAMAM films were placed into a pH 7.0 buffer containing the proteins. Taking Mb as an example, CV scans revealed the growth of the reversible peaks at about −0.34 V with soaking times, indicating that Mb can enter the PAMAM films from its solution. However, the process of Mb entering the PAMAM films was much slower compared with other polymer films [9,41]. About 12 days were needed for PAMAM films to be fully loaded with Mb and to reach the CV steady state. A similar situation was observed for Hb and HRP but with 9 and 6 days for full loading into the PAMAM films, respectively. When fully loaded Mb-PAMAM films were removed from the Mb solution, and transferred to a buffer containing no Mb at the same pH, the CV responses were identical to those in Mb solutions and also quite stable, indicating a strong interaction between Mb and PAMAM. Both cast and immersing methods showed very similar peak positions for protein-PAMAM films at the steady state, but the former was more convenient and quantitative, and thus was used for preparing protein-PAMAM films for the following studies.

At pH 7.0, protonated PAMAM possesses positive surface charges [28]. Cat is negatively charged at pH 7.0 with its isoelectric point at pH 5.8 (Table 1). With the isoelectric point at pH 7.4 for Hb and pH 6.8 for Mb (Table 1), both Hb and Mb are essentially neutral with

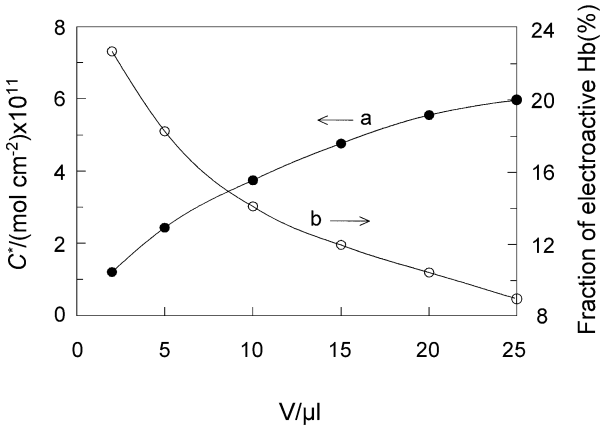

Fig. 2. Dependence of (a) surface concentration of electroactive Hb (C^*) and (b) fractions of electroactive Hb among the total deposited Hb for Hb-PAMAM films on different amounts of Hb-PAMAM (μl) with the constant volume ratio of Hb/PAMAM.

little surface charge at pH 7.0. HRP has its isoelectric point at pH 8.9 (Table 1), and is positively charged at pH 7.0. Thus, if only the overall or net surface charge situation were considered, it would be impossible for the electrostatic attraction to become the predominant interaction between Hb, Mb, or HRP and PAMAM. However, on the surface of the heme proteins, there are lots of aspartic acid (Asp) and glutamic acid (Glu) residues with the carboxyl group as a side chain. The pK_a values of different Asp and Glu side chains are different depending on the type and position of the amino acid residue, but most of them are in the range of pH 2–4 [42–44]. Thus, at pH 7.0, there are still a quite number of negatively charged Asp and Glu groups on the protein surface. The localized electrostatic attraction between the negatively charged Asp and Glu groups of the proteins and the positively charged PAMAM nanoparticles could be the main driving force for the proteins to enter PAMAM films. Recently, secondary or short-range driving forces such as hydrophobic interaction and hydrogen bonding have received more recognition in the film assembly [45]. However, it seems unlikely that hydrophobic interaction becomes a predominant driving force for the proteins to get into PAMAM films, since both the proteins and PAMAM are water-soluble, demonstrating very hydrophilic characters, especially on their surface. PAMAM dendrimers have lots of $-^{+}NH_3$ groups on their surface at pH 7.0, and the proteins have many surface groups containing O and N in their side chains of polypeptide residues. Thus, the hydrogen bonding of N—H···O and N—H···N between PAMAM and the proteins would be probable. This hydrogen bonding, combined with the localized electrostatic interaction, would be mainly responsible for the excellent stability of Hb-, Mb-, and HRP-PAMAM films in blank buffers. Further studies on the interaction between PAMAM and proteins are needed and are underway in our laboratory.

3.3. Influence of the film thickness

The average surface concentration of electroactive proteins in the films (Γ^*) was estimated by using the integrals of CV reduction peaks (Q) and Faraday's law ($Q = nFA\Gamma^*$) [40]. The fractions of electroactive proteins among the total deposited proteins in the protein-PAMAM films were different for different protein films, ranging from 0.8% to 14% (Table 1).

To explain the reason why the fractions of electroactive proteins in protein-PAMAM films were relatively small, the influence of film thickness was investigated. Taking Hb-PAMAM films as an example, various amounts of Hb-PAMAM solutions with the same Hb/PAMAM ratio were deposited on PG electrodes to make Hb-PAMAM films with different film thickness, and CVs were performed to obtain the values of Q and Γ^*. Results showed that while the Γ^* value increased with the film thickness, the fraction of electroactive Hb decreased dramatically (Fig. 2). This implies that only those Hb molecules in the inner layers of the films closest to the electrode surface are electrochemically addressable. This also explains the fact that while about 11% of total deposited Hb in Hb-PAMAM films were lost in the first few minutes of soaking in buffers, the CV reduction peak current remained stable and did not show any decrease during the same testing period.

3.4. Influence of pH on voltammetry

CVs of protein-PAMAM films showed a strong dependence on pH of external buffers. Both reduction and oxidation peak potentials of the heme Fe(III)/Fe(II) redox couple for the four protein-PAMAM films shifted negatively with an increase in pH. The formal potential ($E^{\circ\prime}$) showed a linear dependence on pH in the range of pH 5.0 to 11.0 with a slope of -49.2 mV pH^{-1} for Hb-PAMAM films, -50.2 mV pH^{-1} for Mb-PAMAM films, and -49.6 mV pH^{-1} for HRP-PAMAM films (Fig. 3). While Cat-PAMAM films showed the linear range in pH 2.5–8.0 with a slope of

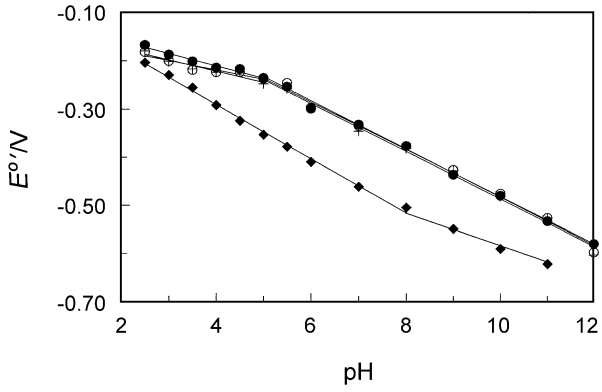

Fig. 3. Influence of pH on the formal potentials estimated by CV at 0.2 V s^{-1} for Hb-PAMAM (●), Mb-PAMAM (○), HRP-PAMAM (+), and Cat-PAMAM films (♦).

-56.4 mV pH^{-1} (Fig. 3). All these slope values are reasonably close to the theoretical value of -57.6 mV pH^{-1} at 18 °C for a one-proton coupled, reversible single-electron transfer [46], which can be represented as

$$\text{HemeFe(III)} + H^+ + e^- \Leftrightarrow \text{HemeFe(II)}$$

For Hb-, Mb-, and HRP-PAMAM films, an inflection point was observed at pH 5.0 in the $E^{\circ\prime}$–pH plot, respectively (Fig. 3). At pH < 5.0, the variation of $E^{\circ\prime}$ with pH showed a much smaller slope, suggesting that the protonatable site of proteins associated with the electrode reaction has an apparent pK_a value of 5.0 [7,42]. For Cat-PAMAM films, however, the $E^{\circ\prime}$–pH relationship showed a different behavior. The inflection point appeared at pH 8.0. At pH > 8.0, the $E^{\circ\prime}$ value shifted with pH with a smaller slope (Fig. 3). The distinct difference in $E^{\circ\prime}$–pH plot for Cat from the other proteins in PAMAM films was also observed in chitosan films [12].

3.5. Estimation of electrochemical parameters

SWV is a powerful method for characterizing the electrochemistry of interfacially confined redox molecules [47,48], and was used here to estimate the average apparent heterogeneous electron transfer rate constant (k_s) and formal potential ($E^{\circ\prime}$) for protein-PAMAM films. The procedure employed nonlinear regression analysis of SWV forward and reverse curves, using a model that combines the single-species surface-confined SWV model [48] with the formal potential distribution model, as described in detail previously [7,49].

The analysis of SWV data for protein-PAMAM films showed accuracy of fit on the 5-$E^{\circ\prime}$ dispersion model over a range of amplitudes and frequencies. Fig. 4 shows an example of SWV forward and reverse curves for Mb-PAMAM films and the fitting results at different frequencies with background subtracted. The simulated curves fit nicely with the experimental data over a range of pulse amplitudes and frequencies. The average k_s and $E^{\circ\prime}$ values obtained by this method at pH 7.0 for the four protein-PAMAM films are listed in Table 2. Although the k_s values for various protein-PAMAM films are different, they are in the same relatively large magnitude of order, showing that the electron transfer of proteins in the PAMAM films was fairly facile. The $E^{\circ\prime}$ value obtained by SWV was in good agreement with that estimated by CV, but different from that for the same protein in clay [21] or chitosan [12] films (Table 2). $E^{\circ\prime}$ of heme Fe(III)/Fe(II) couple of Mb in didodecyldimethylammonium bromide (DDAB) films at pH 7.5 was at +0.05 V vs. NHE (−0.19 V vs. SCE) [50], while in solution phase, the formal potential of Mb at pH 7.0 was estimated to be +0.059 V vs. NHE (−0.18 V vs. SCE) by spectroelectrochemistry [51], all different from that of Mb-PAMAM films. These confirm a specific influence of the film environment on $E^{\circ\prime}$ for heme proteins, as reported previously [7,9]. The film microenvironment and various film components may influence the formal potentials via interactions with the protein or by their effect on the electrode double layer.

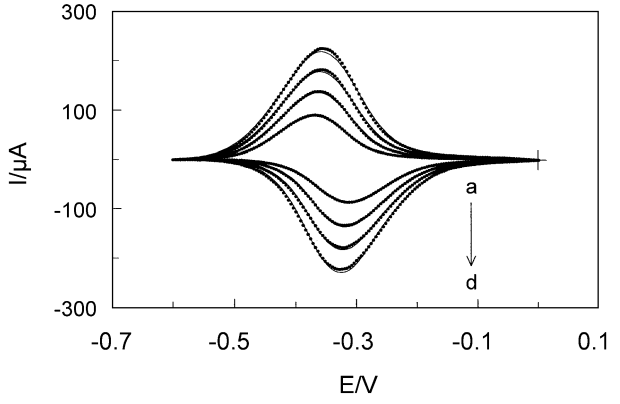

Fig. 4. Square wave forward and reverse current voltammograms for Mb-PAMAM films in pH 7.0 buffer solutions at different frequencies. Points represent the experimental SWVs from which the background has been subtracted. The solid lines are the best fit by nonlinear regression onto the 5-$E^{\circ\prime}$ dispersion model. SWV conditions: pulse height 75 mV, step height 4 mV, and frequencies (Hz): (a) 100, (b) 125, (c) 152, (d) 179.

Table 2
Apparent heterogeneous electron transfer rate constants (k_s) and formal potentials ($E^{\circ\prime}$) for protein films on PG electrodes in pH 7.0 buffers

Films	k_s/s^{-1}	Average $E^{\circ\prime}$/V, vs. SCE		Reference
		CV	SWV	
Hb-PAMAM	47 ± 6	−0.332	−0.337	this work[a]
Mb-PAMAM	57 ± 6	−0.339	−0.337	this work[a]
HRP-PAMAM	77 ± 21	−0.341	−0.341	this work[a]
Cat-PAMAM	23 ± 3	−0.469	−0.471	this work[a]
Hb-Chitosan	104 ± 34	−0.337	−0.344	12
Mb-Chitosan	82 ± 22	−0.330	−0.315	12
HRP-Chitosan	106 ± 34	−0.332	−0.332	12
Cat-Chitosan	40 ± 7	−0.458	−0.467	12
Hb-clay	31 ± 2	−0.347	−0.360	21
Mb-clay	50 ± 3	−0.342	−0.358	21
HRP-clay	74 ± 5	−0.364	−0.363	21

[a] Average values for analysis of eight SWVs at frequencies of 100–180 Hz, amplitudes of 60–75 mV, and a step height of 4 mV.

3.6. Conformational studies

Infrared spectroscopy can provide detailed information on the secondary structure of proteins [52,53], and RAIR spectroscopy was used to detect possible conformational change of the proteins in PAMAM films. We focused on the region of 1700–1500 cm^{-1} where the characteristic amide I band at 1700–1600 cm^{-1} is caused by C=O stretching vibrations of peptide linkage, and the characteristic amide II band at 1600–1500 cm^{-1} results from a combination of N–H in-plane bending and C–N stretching of the peptide groups. Since PAMAM films also showed IR absorbance in

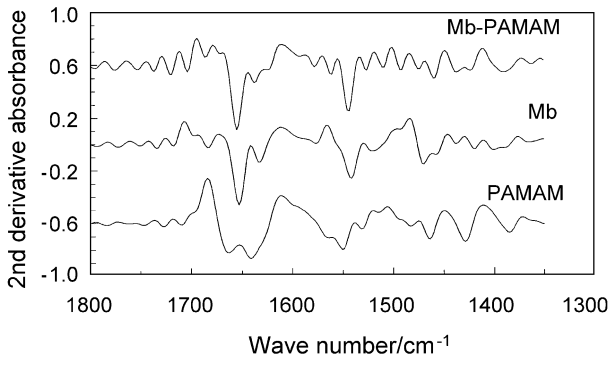

Fig. 5. Second derivative RAIR spectra of PAMAM, Mb, and Mb-PAMAM films. The *y*-axis coordinate only reflects relative value.

the same region, the second derivative RAIR spectra were used to enhance the peak resolution. Take the Mb system as an example (Fig. 5). The second derivative RAIR spectra of Mb-PAMAM films showed the negative peaks of amide I band at 1654 cm^{-1} and amide II band at 1543 cm^{-1}, very similar to those of Mb films alone, respectively, suggesting that Mb essentially retains its native secondary structure in PAMAM films. Similar results were also observed for other protein-PAMAM film systems.

Positions of the Soret absorption band of the heme prosthetic group of the heme proteins may provide some conformational information of the proteins, especially in the heme group region [54,55]. UV–vis spectroscopy was used to detect the dependence of Soret band position on pH of external solution for protein-PAMAM films. For example, when Hb-PAMAM films cast on glass slides were placed into buffers at pH between 5.5 and 11.0, the Soret band at 410 nm was very close to that at 412 nm for dry Hb-PAMAM films and dry Hb films alone (Fig. 6). These results indicate that Hb in PAMAM films essentially retain the secondary structure similar to its native state in the medium pH range. At pH 4.5, the Soret band became broader and much smaller, suggesting that Hb in PAMAM films may denature to a considerable extent when the solution pH shifted toward the acidic direction. Mb-PAMAM films demonstrated UV–vis spectroscopic behavior very similar to Hb-PAMAM films. However, since HRP- and Cat-PAMAM films on glass slides were not stable in solution, it was difficult to conduct the experiments of pH effect with UV–vis spectroscopy for the HRP- and Cat-PAMAM films.

3.7. Catalytic reactivity

The electrocatalytic behavior of protein-PAMAM films toward various substrates was characterized by CV. Qualitatively, Cat-PAMAM films exhibited the catalytic properties similar to the other protein-PAMAM films, however, since Cat-PAMAM films were not very stable in solution, it was difficult to obtain the quantitative estimation. Thus, the electrocatalytic studies were mainly focused on Hb-, Mb-, and HRP-PAMAM films.

Electrochemical catalytic reduction of oxygen was observed at protein-PAMAM film electrodes. When a certain volume of air was passed through a pH 7.0 oxygen-free buffer using a syringe, significant increases in reduction peak at about −0.3 V were observed for Hb-, Mb-, and HRP-PAMAM films (Fig. 7) compared with those in the absence of oxygen. This increase in reduction peak was accompanied by the disappearance of oxidation peak for heme Fe(II), since heme Fe(II) had reacted with oxygen. An increase in the amount of oxygen in solution led to the increase of the reduction peak currents. For PAMAM films with no protein incorporated, a wave for direct reduction of oxygen was observed at about −0.8 V (Fig. 7b), far more negative than the potential of the catalytic reduction peaks. Thus, the heme proteins in PAMAM films decreased the reduction overpotential of oxygen by about 0.5 V. The catalytic efficiency, expressed as the ratio of reduction peak current of heme proteins in the presence (I_c) and absence of oxygen (I_d), I_c/I_d, decreased with an increase of scan rate (Fig. 7, inset). All these results are characteristic of the reduction of oxygen by electrochemical catalysis with protein-PAMAM films [56,57]. With the same volume of air injected and at the same CV scan rate, the three protein-PAMAM films showed different catalytic reduction peak currents with an order of Mb>Hb>HRP (Fig. 7), while the catalytic efficiency for the protein-PAMAM films exhibited

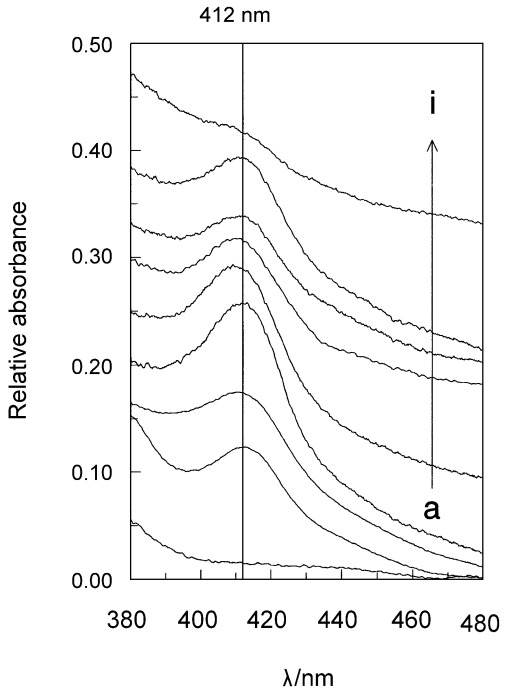

Fig. 6. UV–vis absorption spectra of (a) dry PAMAM, (b) dry Hb, and (c) dry Hb-PAMAM films, and Hb-PAMAM films in different pH buffers: (d) pH 5.5, (e) pH 7.0, (f) pH 9.0, (g) pH 10.0, (h) pH 11.0, (i) pH 4.0.

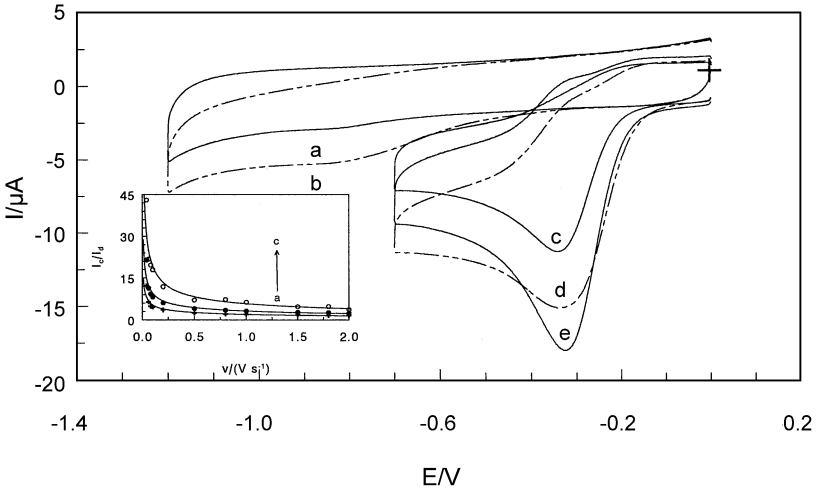

Fig. 7. Cyclic voltammograms at 0.2 V s^{-1} in 5 ml of pH 7.0 buffers for (a) PAMAM films with no oxygen present, and for (b) PAMAM, (c) HRP-PAMAM, (d) Hb-PAMAM, (e) Mb-PAMAM films after 40 ml of air was injected into a sealed cell, respectively. Inset: influence of scan rate on catalytic efficiency, I_c/I_d, for (a) Hb-PAMAM, (b) Mb-PAMAM, (c) HRP-PAMAM film in pH 7.0 buffers, where I_d is the CV reduction peak current in buffers without oxygen and I_c is the CV reduction peak current in 10 ml of buffers with 40 ml of air injected.

a different sequence of HRP>Mb>Hb (Fig. 7, inset; and Table 3).

The electrochemical catalysis of hydrogen peroxide at protein-PAMAM film electrodes were also tested by CV. Taking HRP-PAMAM films as an example, when H_2O_2 was added to a pH 5.5 buffer, compared with the system with no H_2O_2 present (Fig. 8c), a significant increase of the reduction peak at about −0.30 V was observed with the disappearance of the oxidation peak (Fig. 8d). The reduction peak current increased with the concentration of H_2O_2 in solution (Fig. 8e). However, direct reduction of H_2O_2 at blank PAMAM film electrodes was not observed in the studied potential window (Fig. 8b). The linear relationship between the electrocatalytic reduction peak current and H_2O_2 concentration was observed between 0.02 and 0.16 mM, while at higher H_2O_2 concentrations, the CV response showed a level-off tendency. The plots of I_{pc} vs. concentration of H_2O_2 for Hb- and Mb-PAMAM films showed shapes very similar to that of HRP-PAMAM films but with a little different linear ranges. The catalytic reduction of H_2O_2 at HRP-PAMAM film electrodes showed the peak position and shape very similar to those of oxygen (Figs. 7 and 8), implying the similarity of reaction mechanism between the two systems. This was also observed for other protein films and discussed in detail in previous publications [37,58].

Catalytic reduction of nitrite was also studied at protein-PAMAM film electrodes. For example, with Hb-PAMAM films, a new reduction peak appeared at about −0.70 V when NO_2^- was added in a pH 5.5 buffer (Fig. 9), and the peak increased with a further addition of NO_2^-. Direct reduction of NO_2^- on PAMAM films with no Hb present was found at the potential more negative than −1.2 V. Thus, Hb-PAMAM films decreased the reduction overpotential of NO_2^- by at least 0.5 V. Although the clear elucidation for the reduction mechanism of NO_2^- on Hb-PAMAM films is not yet known and further studies are needed, the reduction product at −0.70 V is probably N_2O, which was detected previously by mass spectroscopy with

Table 3
Catalytic efficiency (I_c/I_d), or detection limit for different substrates at protein-PAMAM film electrodes

Films	Catalytic efficiency (I_c/I_d)		Detection limit/mM
	O_2[a]	H_2O_2[b]	$NaNO_2$[c]
Hb-PAMAM	3.6	5.0	0.40
Mb-PAMAM	6.2	7.6	0.80
HRP-PAMAM	11.9	10.9	0.80

[a] From CV at 0.2 V s^{-1} in pH 7.0 buffers. 40 ml of air was passed in 10 ml solution.
[b] From CV at 0.2 V s^{-1} and with 0.12 mM H_2O_2 in pH 5.5 buffers.
[c] From CV at 0.1 V s^{-1} in pH 5.5 buffers.

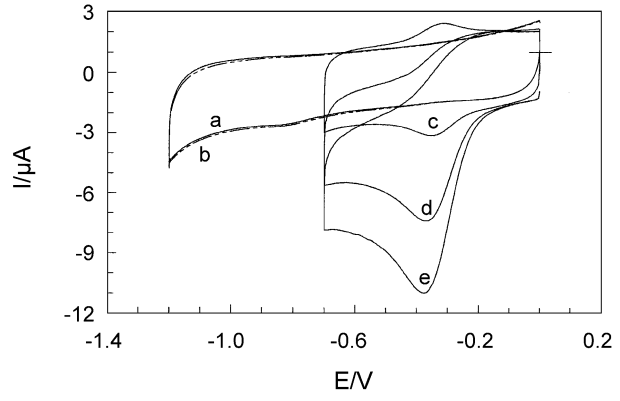

Fig. 8. Cyclic voltammograms at 0.2 V s^{-1} in pH 7.0 buffers for (a) PAMAM films in buffers containing no H_2O_2, (b) PAMAM films in buffers containing 0.08 mM H_2O_2, (c) HRP-PAMAM films in buffers containing no H_2O_2, (d) HRP-PAMAM films in buffers containing 0.04 mM H_2O_2, (e) HRP-PAMAM films in buffers containing 0.08 mM H_2O_2.

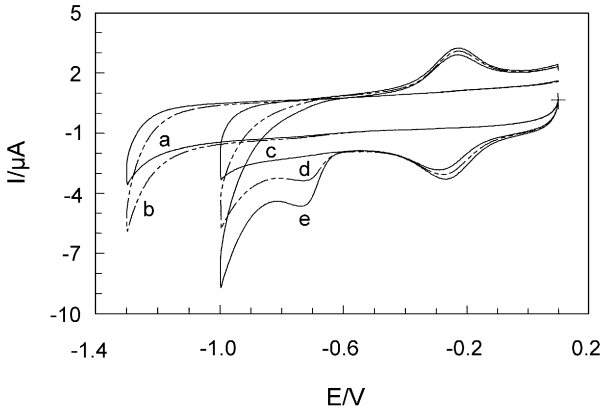

Fig. 9. Cyclic voltammograms at 0.1 V s^{-1} in pH 5.5 buffers for (a) PAMAM films in buffers containing no $NaNO_2$, (b) PAMAM films in buffers containing 6 mM $NaNO_2$, (c) Hb-PAMAM films in buffers containing no $NaNO_2$, (d) Hb-PAMAM films in buffers containing 6 mM $NaNO_2$, (e) Hb-PAMAM films in buffers containing 16.5 mM $NaNO_2$.

Mb-DDAB films on electrolysis at -0.895 V in pH 7.4 buffers [59]. The catalysis of NO_2^- with protein-PAMAM films was also used to determine the concentration of nitrite in solution. While the linear ranges of calibration curves were a little different depending on different protein-PAMAM films, they were similar and approximately from 1 to 10 mM.

Catalytic efficiencies for O_2 and H_2O_2 with the three protein-PAMAM films are also listed in Table 3 for comparison. The catalytic reduction peak potential of NO_2^- at protein-PAMAM film electrodes is at about -0.7 V, very different from that of protein-PAMAM films in the absence of NO_2^- (Fig. 9), and the ratio of I_c/I_d cannot be defined in this case. Thus, the detection limit values are listed in Table 3 for comparison with the NO_2^- system. For the substrates of oxygen and hydrogen peroxide, Mb and Hb generally demonstrate similar catalytic behavior, while HRP seems the most active among the three in PAMAM films. For the nitrite system, however, Hb-PAMAM films seem to be more sensitive than the other protein films in the catalytic reductions.

4. Conclusions

The nanosized organic PAMAM has a unique structure, and demonstrates excellent properties such as good biocompatibility and high surface activity. The PAMAM films thus provide a favorable microenvironment for immobilized heme proteins, and the proteins in PAMAM films exhibit good electroactivity and retain their near-native secondary structures in the medium pH range. The localized electrostatic interaction between the proteins and PAMAM, as well as the hydrogen bonding, may greatly strengthen the stability of protein-PAMAM films in solution, although Cat shows different redox potential and less stability compared with other proteins in PAMAM films. The heme proteins in PAMAM films also show good electrocatalytic activity toward various substrates with biological or environmental significance. The significant decrease of potentials required for reduction of these substrates, combined with good stability of the films, suggests that the protein-PAMAM films might be useful for practical applications in constructing biosensors or bioreactors based on the direct electrochemistry of enzyme without using any mediator.

Acknowledgements

The financial support from the National Natural Science Foundation of China (20275006 and 29975003) is acknowledged.

References

[1] F.A. Armstrong, F.S. Wilson, Recent developments in Faradaic bioelectrochemistry, Electrochim. Acta 45 (2000) 2623–2645.
[2] J.F. Rusling, Z. Zhang, Biomolecules, Biointerfaces, and Applications, in: R.W. Nalwa (Ed.), Handbook of Surfaces and Interfaces of Materials, vol. 5, Academic, San Diego, 2001, pp. 33–71.
[3] J.F. Rusling, Enzyme bioelectrochemistry in cast biomembrane-like films, Acc. Chem. Res. 31 (1998) 363–369.
[4] J.B. Schenkman, H. Grei, Cytochrome P450, Springer, Berlin, 1993.
[5] N. Hu, Direct electrochemistry of redox proteins or enzymes at various film electrodes and their possible applications in monitoring some pollutants, Pure Appl. Chem. 73 (2001) 1979–1991.
[6] L. Gorton, A. Lindgren, T. Larsson, F.D. Munteanu, T. Ruzgas, I. Gazaryan, Direct electron transfer between heme-containing enzymes and electrodes as basis for third generation biosensors, Anal. Chim. Acta 400 (1999) 91–108.
[7] A.-E.F. Nassar, Z. Zhang, N. Hu, J.F. Rusling, T.F. Kumosinski, Proton-coupled electron transfer from electrodes to myoglobin in ordered biomembrane-like films, J. Phys. Chem., B. 101 (1997) 2224–2231.
[8] J. Yang, N. Hu, Direct electron transfer for hemoglobin in biomembrane-like dimyristoyl phosphatidylcholine films on pyrolytic graphite electrodes, Bioelectrochem. Bioenerg. 48 (1999) 117–127.
[9] N. Hu, J.F. Rusling, Electrochemistry and catalysis with myoglobin in hydrated poly(ester sulfonic acid) ionomer films, Langmuir 13 (1997) 4119–4125.
[10] H. Sun, N. Hu, H. Ma, Direct electrochemistry of hemoglobin in polyacrylamide hydrogel films on pyrolytic graphite electrodes, Electroanalysis 12 (2000) 1064–1070.
[11] H. Lu, Z. Li, N. Hu, Direct voltammetry and electrocatalytic properties of catalase incorporated in polyacrylamide hydrogel films, Biophys. Chemist. 104 (2003) 623–632.
[12] H. Huang, N. Hu, Y. Zeng, G. Zhou, Electrochemistry and electrocatalysis with heme proteins in chitosan biopolymer films, Anal. Biochem. 308 (2002) 141–151.
[13] H. Liu, N. Hu, Heme protein-gluten films: voltammetric studies and their electrocatalytic properties, Anal. Chim. Acta 481 (2003) 91–99.
[14] H. Sun, H. Ma, N. Hu, Electroactive hemoglobin-surfactant-polymer biomembrane-like films, Bioelectrochem. Bioenerg. 49 (1999) 1–10.
[15] Y. Hu, N. Hu, Y. Zeng, Electrochemistry and electrocatalysis with myoglobin in biomembrane-like surfactant-polymer $2C_{12}N^+PA^-$ composite films, Talanta 50 (2000) 1183–1195.
[16] X. Chen, N. Hu, Y. Zeng, J.F. Rusling, J. Yang, Ordered electrochemi-

cally-active films of hemoglobin, didodecyldimethylammonium ions and clay, Langmuir 15 (1999) 7022–7030.
[17] H. Ma, N. Hu, J.F. Rusling, Electroactive myoglobin films grown layer-by-layer with poly(styrenesulfonate) on pyrolytic graphite electrodes, Langmuir 16 (2000) 4969–4975.
[18] L. Wang, N. Hu, Direct electrochemistry of hemoglobin in layer-by-layer films with poly(vinyl sulfonate) grown on pyrolytic graphite electrodes, Bioelectrochemistry 53 (2001) 205–212.
[19] P. He, N. Hu, G. Zhou, Assembly of electroactive layer-by-layer films of hemoglobin and polycationic poly(diallyldimethyl ammonium), Biomacromolecules 3 (2002) 139–146.
[20] Y. Lvov, B. Munge, O. Giraldo, I. Ichinose, S. Suib, J.F. Rusling, Films of manganese oxide nanoparticles with polycations or myoglobin from alternate-layer adsorption, Langmuir 16 (2000) 8850–8857.
[21] Y. Zhou, N. Hu, Y. Zeng, J.F. Rusling, Heme protein-clay films: direct electrochemistry and electrochemical catalysis, Langmuir 18 (2002) 211–219.
[22] Y. Zhou, Z. Li, N. Hu, Y. Zeng, J.F. Rusling, Layer-by-layer assembly of ultrathin films of hemoglobin and clay nanoparticles with electrochemical and catalytic activity, Langmuir 18 (2002) 8573–8579.
[23] D.A. Tomalia, A.M. Naylor, W.A. Goddard, Starburst dendrimers: molecular-level control of size, shape, surface chemistry, topology, and flexibility from atoms to macroscopic matter, Angew. Chem., Int. Ed. Engl. 29 (1990) 138–175.
[24] M. Fischer, F. Vogtle, Dendrimer: from design to application—a progress report, Angew. Chem., Int. Ed. Engl. 38 (1999) 884–905.
[25] C.R. Newkome, C.N. Moorefiled, F. Vogtle, Dendritic Molecules. Concepts–Syntheses–Perspectives, Springer, New York, 1996.
[26] D.C. Tully, J.M.J. Frechet, Dendrimers at surfaces and interfaces: chemistry and applications, Chem. Commun. (2001) 1229–1239.
[27] V.V. Tsukruk, F. Rinderspacher, V.N. Bliznyuk, Self-assembled multilayer films from dendrimers, Langmuir 13 (1997) 2171–2176.
[28] W. Chen, D.A. Tomalia, J.L. Thomas, Unusual pH-dependent polarity changes in PAMAM dendrimers: evidence for pH-responsive conformational changes, Macromolecules 33 (2000) 9169–9172.
[29] M.F. Ottaviani, E. Cossu, N. Turro, D.A. Tomalia, Characterization of starburst dendrimers by electron paramagnetic resonance: 2. Positively charged nitroxide radicals of variable chain length used as spin probes, J. Am. Chem. Soc. 117 (1995) 4387–4398.
[30] A.K. Patri, I.J. Majoros, J.R. Baker Jr., Dentritic polymer macromolecular carriers for drug delivery, Curr. Opin. Chem. Biol. 6 (2002) 466–471.
[31] H.C. Yoon, M.Y. Hong, H.S. Kim, Functionalization of a poly(amidoamine) dendrimer with ferrocenyls and its application to the construction of a reagentless enzyme electrode, Anal. Chem. 72 (2000) 4420–4427.
[32] H.C. Yoon, H.S. Kim, Multilayered assembly of dendrimers with enzymes on gold: thickness-controlled biosensing interface, Anal. Chem. 72 (2000) 922–926.
[33] H.C. Yoon, M.Y. Hong, H.S. Kim, Affinity biosensor for avidin using a double functionalized dendrimer monolayer on a gold electrode, Anal. Biochem. 282 (2000) 121–128.
[34] H.C. Yoon, M.Y. Hong, H.S. Kim, Reversible association/dissociation reaction of avidin on the dendrimer monolayer functionalized with a biotin analogue for a regenerable affinity-sensing surface, Langmuir 17 (2001) 1234–1239.
[35] Q. Huang, Z. Lu, J.F. Rusling, Composite films of surfactants, Nafion, and proteins with electrochemical and enzyme activity, Langmuir 12 (1996) 5472–5480.
[36] T. Ferri, A. Poscia, R. Santucci, Direct electrochemistry of membrane-entrapped horseradish peroxidase: Part I. A voltammetric and spectroscopic study, Bioelectrochem. Bioenerg. 44 (1998) 177–181.
[37] Z. Zhang, S. Chouchane, R.S. Magliozzo, J.F. Rusling, Direct voltammetry and catalysis with Mycobacterium tuberculosis catalase-peroxidase, peroxidases, and catalase in lipid films, Anal. Chem. 74 (2002) 163–170.
[38] A.-E.F. Nassar, W.S. Willis, J.F. Rusling, Electron transfer from electrodes to myoglobin: facilitated in surfactant films and blocked by absorbed biomacromolecules, Anal. Chem. 67 (1995) 2386–2392.
[39] S. Stechemesser, W. Eimer, Solvent-dependent swelling of poly(amido amine) starburst dendrimers, Macromolecules 30 (1997) 2204–2206.
[40] R.W. Murray, in: A.J. Bard (Ed.), Electroanalytical Chemistry, vol. 13, Marcel Dekker, New York, 1984, pp. 191–368.
[41] L. Shen, R. Huang, N. Hu, Myoglobin in polyacrylamide hydrogel films: direct electrochemistry and electrochemical catalysis, Talanta 56 (2002) 1131–1139.
[42] A.-S. Yang, B. Honig, Structural origins of pH and ionic strength effects on protein stability, Acid denaturation of sperm whale apomyoglobin, J. Mol. Biol. 237 (1994) 602–614.
[43] S.J. Shire, G.I.H. Hanania, F.R.N. Gurd, Electrostatic effects in myoglobin. Hydrogen ion equilibria in sperm whale ferrimyoglobin, Biochemistry 13 (1974) 2967–2979.
[44] J.B. Matthew, G.I.H. Hanania, F.R.N. Gurd, Electrostatic effects in hemoglobin: hydrogen ion equilibria in human deoxy- and oxyhemoglobin A, Biochemistry 18 (1979) 1919–1928.
[45] P. Hammond, Recent explorations in electrostatic multilayer thin film assembly, Curr. Opin. Colloid Interface Sci. 6 (1999) 430–442.
[46] A.M. Bond, Modern Polarographic Methods in Analytical Chemistry, Marcel Dekker, New York, 1980.
[47] J.G. Osteryoung, J.J. O'Dea, Square-wave Voltammetry, in: A.J. Bard (Ed.), Electroanalytical Chemistry, vol. 14, Marcel Dekker, New York, 1986, pp. 209–325.
[48] J.J. O'Dea, J.G. Osteryoung, Characterization of quasi-reversible surface processes by square-wave voltammetry, Anal. Chem. 65 (1993) 3090–3097.
[49] Z. Zhang, J.F. Rusling, Electron transfer between myoglobin and electrodes in thin films of phosphatidylcholines and dihexadecylphosphate, Biophys. Chemist. 63 (1997) 133–146.
[50] J.F. Rusling, A.-E.F. Nassar, Enhanced electron transfer for myoglobin in surfactant films on electrodes, J. Am. Chem. Soc. 115 (1993) 11891–11897.
[51] B.R. Van Dyke, P. Saltman, F.A. Armstrong, Control of myoglobin electron-transfer rates by the distal (nonbound) histidine residue, J. Am. Chem. Soc. 118 (1996) 3490–3492.
[52] T.F. Kumosinski, J.J. Unruh, in: T.F. Kumosinski, M.N. Liebman (Eds.), Molecular Modeling, ACS Symp. Ser., vol. 576, American Chemical Society, Washington, DC, 1994, pp. 71–73.
[53] D.D. Schlereth, W. Mantele, Redox-induced conformational changes in myoglobin and hemoglobin: electrochemistry and ultraviolet–visible and Fourier transform infrared difference spectroscopy at surface-modified gold electrodes in an ultra-thin-layer spectroelectrochemical cell, Biochemistry 31 (1992) 7494–7502.
[54] H. Theorell, A. Ehrenberg, Spectrophotometric, magnetic, and titrimetric studies on the heme-linked groups in myoglobin, Acta Chem. Scand. 5 (1951) 823–848.
[55] P. George, G. Hanania, Spectrophotometric study of ionizations in methemoglobin, Biochem. J. 55 (1953) 236–243.
[56] C.P. Andrieux, C. Blocman, J.M. Dumas-Bouchiant, J.M. Saveant, Heterogeneous and homogeneous electron transfers to aromatic halides. An electrochemical redox catalysis study in the halobenzene and halopyridine series, J. Am. Chem. Soc. 101 (1979) 3431–3441.
[57] C.P. Andrieux, C. Blocman, J.M. Dumas-Bouchiant, F. M'Halla, J.M. Saveant, Homogeneous redox catalysis of electrochemical reactions: Part V. Cyclic voltammetry, J. Electroanal. Chem. 113 (1980) 19–40.
[58] R. Huang, N. Hu, Direct electrochemistry and electrocatalysis with horseradish peroxidase in Eastman AQ films, Bioelectrochemistry 54 (2001) 75–81.
[59] R. Lin, M. Bayachou, J. Greaves, P.J. Farmer, Nitrite reduction by myoglobin in surfactant films, J. Am. Chem. Soc. 119 (1997) 12689–12690.
[60] A. Bellelli, G. Antonini, M. Brunori, B.A. Springer, S.G. Sligar, Transient spectroscopy of the traction of cyanides with ferrous my-

oglobin-effect of distal side residues, J. Biol. Chem. 265 (1990) 18898–18901.
[61] K.G. Welinder, Amino acid sequence studies of horseradish-peroxidase: 4. Amino and carboxyl termini, cyanogen-bromide and tryptic fragments, the complete sequence, and some structural characteristics of horseradish peroxidase-C, Eur. J. Biochem. 96 (1979) 483–502.
[62] F. Caruso, D. Trau, H. Mohwald, R. Renneberg, Enzyme encapsulation in layer-by-layer engineered polymer multiplayer capsules, Langmuir 16 (2000) 1485–1488.